NACA

RESEARCH MEMORANDUM

for the

U. S. Air Force

CALCULATION OF THE LATERAL STABILITY OF A

DIRECTLY COUPLED TANDEM-TOWED FIGHTER AIRPLANE

AND CORRELATION WITH EXPERIMENTAL DATA

By Robert E. Shanks

Langley Aeronautical Laboratory
Langley Field, Va.

NACA Res abr
+ R N - 148

June 2V, 1958

NATIONAL ADVISORY COMMITTEE
FOR AERONAUTICS
WASHINGTON

CON

NATIONAL ADVISORY COMMITTEE FOR AERONAUTICS

RESEARCH MEMORANDUM

for the

U. S. Air Force

CALCULATION OF THE LATERAL STABILITY OF A

DIRECTLY COUPLED TANDEM-TOWED FIGHTER AIRPLANE

AND CORRELATION WITH EXPERIMENTAL DATA

By Robert E. Shanks

SUMMARY

A theoretical method is presented for predicting the dynamic lateral stability characteristics of an airplane towed in tandem by a much larger airplane. Values of period and time to damp to one-half amplitude and rolling motions calculated by an analog computer have been correlated with results of two experimental investigations conducted in the Langley free-flight tunnel which were part of a U. S. Air Force program (Project FICON) to develop a satisfactory arrangement by which a bomber could tow a parasite fighter. In general, the theoretical results agree with the experimental results.

INTRODUCTION

As part of a U. S. Air Force program (Project FICON) to develop a satisfactory arrangement by which a bomber could tow a parasite fighter, two experimental investigations have been conducted in the Langley free-flight tunnel to determine the dynamic stability characteristics of models of two types of fighter airplanes towed by a bomber. On the basis of the results of these investigations reported in references 1 and 2 and of subsequent full-scale flight tests, a satisfactory tandem directly coupled configuration was selected as the final arrangement. In order to provide a means for predicting the lateral stability characteristics of future directly coupled aircraft configurations of this type, the equations of lateral motion are derived for the towed airplane. The period and damping have been calculated from the characteristic modes of the system and time histories of the rolling motions in response to specified aileron disturbances were also obtained by using this method for the conditions of the

model tests of the Republic F-84E airplane and the Chance Vought
F7U-3 airplane of references 1 and 2, respectively. The results of the
calculations are correlated with the experimental data.

SYMBOLS

All forces and moments are referred to the conventional stability
system of axes (see fig. 1).

W	weight of model, lb
m	mass of model, slugs
S	wing area, sq ft
K	spring constant, ft-lb/radian
b	wing span, ft
t	time, sec
V	airspeed, ft/sec
v	sideslip velocity, ft/sec
q	dynamic pressure, $\frac{1}{2}\rho V^2$, lb/sq ft
ρ	air density, slugs/cu ft
μ	relative-density factor, $m/\rho Sb$
η	angle of attack of principal longitudinal axis of inertia, deg (see fig. 1)
k_{X_O}	radius of gyration about principal longitudinal axis of inertia, ft
k_{Z_O}	radius of gyration about principal normal axis of inertia, ft
k_X	radius of gyration about X-axis, $\sqrt{k_{X_O}^2\cos^2\eta + k_{Z_O}^2\sin^2\eta}$, ft
k_Z	radius of gyration about Z-axis, $\sqrt{k_{Z_O}^2\cos^2\eta + k_{X_O}^2\sin^2\eta}$, ft

k_{XZ} product-of-inertia factor, $\left(k_{X_o}{}^2 - k_{Z_o}{}^2\right) \sin \eta \cos \eta$

$K_X = \dfrac{k_X}{b}$

$K_Z = \dfrac{k_Z}{b}$

$K_{XZ} = \dfrac{k_{XZ}}{b^2}$

x horizontal distance from tow-attachment coupling to center of gravity measured along longitudinal stability axis; values of x must be determined for each angle of attack, ft (see fig. 1)

z vertical distance from tow-attachment coupling to center of gravity measured along normal stability axis; values of z must be determined for each angle of attack, ft (see fig. 1)

A,B,C,D,E coefficients of the stability characteristic equation

λ root of stability characteristic equation

D differential operator, d/ds

s nondimensional time parameter based on span, tV/b

P period of lateral oscillation, sec

$T_{1/2}$ time to damp to one-half amplitude, sec

β angle of sideslip, radians

ψ angle of yaw, radians

ϕ angle of bank, radians

r yawing angular velocity, $d\psi/dt$, radians/sec

p rolling angular velocity, $d\phi/dt$, radians/sec

Y side force, lb

N yawing moment, ft-lb

L   rolling moment, ft-lb

$Y_\beta = \dfrac{\partial Y}{\partial \beta}$

$N_\beta = \dfrac{\partial N}{\partial \beta}$

$L_\beta = \dfrac{\partial L}{\partial \beta}$

$Y_{\dot\psi} = \dfrac{\partial L}{\partial \dot\psi}$

$N_{\dot\psi} = \dfrac{\partial N}{\partial \dot\psi}$

$L_{\dot\psi} = \dfrac{\partial L}{\partial \dot\psi}$

$Y_{\dot\beta} = \dfrac{\partial Y}{\partial \dot\beta}$

$N_{\dot\beta} = \dfrac{\partial N}{\partial \dot\beta}$

$L_{\dot\beta} = \dfrac{\partial L}{\partial \dot\beta}$

C_Y lateral-force coefficient, Y/qS

C_n yawing-moment coefficient, N/qSb

C_l rolling-moment coefficient, L/qSb

$C_{Y_\beta} = \dfrac{\partial C_Y}{\partial \beta}$

$C_{l_\beta} = \dfrac{\partial C_l}{\partial \beta}$

$C_{n_\beta} = \dfrac{\partial C_n}{\partial \beta}$

$C_{Y_p} = \dfrac{\partial C_Y}{\partial \frac{pb}{2V}}$

$$C_{n_p} = \frac{\partial C_n}{\partial \frac{pb}{2V}}$$

$$C_{l_p} = \frac{\partial C_l}{\partial \frac{pb}{2V}}$$

$$C_{Y_r} = \frac{\partial C_Y}{\partial \frac{rb}{2V}}$$

$$C_{n_r} = \frac{\partial C_n}{\partial \frac{rb}{2V}}$$

$$C_{l_r} = \frac{\partial C_l}{\partial \frac{rb}{2V}}$$

$$C_{Y_{\dot{\beta}}} = \frac{\partial C_Y}{\partial \frac{\dot{\beta}b}{2V}}$$

$$C_{n_{\dot{\beta}}} = \frac{\partial C_n}{\partial \frac{\dot{\beta}b}{2V}}$$

$$C_{l_{\dot{\beta}}} = \frac{\partial C_l}{\partial \frac{\dot{\beta}b}{2V}}$$

C_W weight coefficient, W/qS

C_K spring-constant coefficient, $K/\rho SV^2 b$

Subscripts:

c   constraint

o   control or initial

THEORETICAL METHOD

Assumptions of the Analysis

In addition to the customary assumptions of small disturbances and linear derivatives, the following assumptions were also made:

The motions of the towing airplane arising from the fighter motions are assumed to be negligible because of the large difference in the relative size of the two airplanes, and the towing airplane is assumed to remain in steady level flight.

The fighter airplane is assumed to be rigid, and it is assumed that the tow-attachment coupling is mounted to the towing airplane without flexibility; therefore, elastic effects may be ignored.

The air flow in the vicinity of the fighter is assumed to be smooth and unaffected by the towing airplane.

Equations of Motion

The equations of motion of the towed airplane were developed by using Lagrange's method of undetermined multipliers as a means of taking account of the constraint on the airplane. This method is based on d'Alembert's principle and is discussed in detail in reference 3.

The equation of condition which defines the sidewise velocity at the constraint or tow-attachment coupling is

$$v_c = v + V\psi + x\dot{\psi} - z\dot{\phi} = 0 \tag{1}$$

Solving for the sidewise velocity of the airplane center of gravity from equation (1) results in

$$v = z\dot{\phi} - x\dot{\psi} - V\psi \tag{2}$$

and

$$\dot{v} = z\ddot{\phi} - x\ddot{\psi} - V\dot{\psi} \tag{3}$$

The lateral equations of the free airplane are:

Side-force equation,

$$m(\dot{v} + V\dot{\psi}) = Y_{\dot{\beta}}\frac{\dot{v}}{V} + Y_{\beta}\frac{v}{V} + Y_{\dot{\psi}}\dot{\psi} + Y_{\dot{\phi}}\dot{\phi} + W\phi + Y_o = Y \tag{4}$$

Yawing-moment equation,

$$I_Z\ddot{\psi} - I_{XZ}\ddot{\phi} = N_{\dot\beta}\frac{\dot{v}}{V} + N_{\dot\psi}\dot{\psi} + N_{\dot\phi}\dot{\phi} + N_\beta\frac{v}{V} + N_O = N \qquad (5)$$

Rolling-moment equation,

$$I_X\ddot{\phi} - I_{XZ}\ddot{\psi} = L_{\dot\beta}\frac{\dot{v}}{V} + L_{\dot\psi}\dot{\psi} + L_{\dot\phi}\dot{\phi} + L_\beta\frac{v}{V} + K_\phi\phi + L_O = L \qquad (6)$$

Use of d'Alembert's principle and the Lagrange multipliers results in the following equation:

$$\left[m(\dot{v} + V\dot{\psi}) - Y\right]\delta y + \left[I_Z\ddot{\psi} - I_{XZ}\ddot{\phi} - N\right]\delta\psi +$$

$$\left[I_X\ddot{\phi} - I_{XZ}\ddot{\psi} - L\right]\delta\phi + \lambda\left[\delta y + x\,\delta\psi - z\,\delta\phi\right] = 0 \qquad (7a)$$

or

$$\left[m(\dot{v} + V\dot{\psi}) - Y + \lambda\right]\delta y + \left[I_Z\ddot{\psi} - I_{XZ}\ddot{\phi} - N + x\lambda\right]\delta\psi +$$

$$\left[I_X\ddot{\phi} - I_{XZ}\ddot{\psi} - L - z\lambda\right]\delta\phi = 0 \qquad (7b)$$

Because of the inclusion of λ, the virtual displacements δy, $\delta\psi$, and $\delta\phi$ are arbitrary and, therefore, the coefficients of each displacement must vanish. Then, solving for λ from the coefficient of δy yields

$$\lambda = Y - m(\dot{v} + V\dot{\psi}) \qquad (8)$$

Substituting for λ and for v and $\dot{v}$ from equations (2) and (3) in the yawing-moment and rolling-moment equations gives

$$I_Z\ddot{\psi} - I_{XZ}\ddot{\phi} - \frac{1}{V}N_{\dot\beta}(z\ddot{\phi} - x\ddot{\psi} - V\dot{\psi}) - N_{\dot\psi}\dot{\psi} - N_{\dot\phi}\dot{\phi} - \frac{1}{V}N_\beta(z\dot{\phi} - x\dot{\psi} - V\psi) +$$

$$x\left[\frac{1}{V}Y_{\dot\beta}(z\ddot{\phi} - x\ddot{\psi} - V\dot{\psi}) + \frac{1}{V}Y_\beta(z\dot{\phi} - x\dot{\psi} - V\psi) + Y_{\dot\psi}\dot{\psi} + Y_{\dot\phi}\dot{\phi} + W\phi -\right.$$

$$\left.m(z\ddot{\phi} - x\ddot{\psi} - V\dot{\psi}) - mV\dot{\psi}\right] = N_O - xY_O \qquad (9)$$

$$I_X \ddot{\phi} - I_{XZ} \ddot{\psi} - \frac{1}{V} L_{\dot{\beta}}(z\ddot{\phi} - x\ddot{\psi} - V\dot{\psi}) - L_{\dot{\psi}}\dot{\psi} - L_{\dot{\phi}}\dot{\phi} - \frac{1}{V} L_{\beta}(z\dot{\phi} - x\dot{\psi} - V\psi) -$$

$$K_{\phi}\phi - z\left[\frac{1}{V} Y_{\dot{\beta}}(z\ddot{\phi} - x\ddot{\psi} - V\dot{\psi}) + \frac{1}{V} Y_{\beta}(z\dot{\phi} - x\dot{\psi} - V\psi) + Y_{\dot{\psi}}\dot{\psi} + Y_{\dot{\phi}}\dot{\phi} + \right.$$

$$\left. W\phi - m(z\ddot{\phi} - x\ddot{\psi} - V\dot{\psi}) - mV\dot{\psi}\right] = L_O + zY_O \tag{10}$$

These equations may be expressed in nondimensional form by dividing each
by $\frac{1}{2}\rho S V^2 b$ and by using the following relationships and the operator D:

$$\mu = \frac{m}{\rho S b}$$

$$K_X = \frac{k_X}{b} \qquad\qquad\qquad D = \frac{d}{ds}$$

$$K_Z = \frac{k_Z}{b} \qquad\qquad\qquad ds = \frac{V}{b} dt$$

$$K_{XZ} = \frac{k_{XZ}}{b^2}$$

The equations in nondimensional form are:

Yawing-moment equation,

$$\left[2\mu K_Z^2 + 2\mu\left(\frac{x}{b}\right)^2 + \frac{1}{2}\frac{x}{b} C_{n_{\dot{\beta}}} - \frac{1}{2}\left(\frac{x}{b}\right)^2 C_{Y_{\dot{\beta}}}\right]D^2\psi + \left[\frac{1}{2} C_{n_{\dot{\beta}}} - \frac{1}{2}\frac{x}{b} C_{Y_{\dot{\beta}}} - \frac{1}{2} C_{n_r} + \right.$$

$$\left. \frac{1}{2}\frac{x}{b} C_{Y_r} + \frac{x}{b} C_{n_{\beta}} - \left(\frac{x}{b}\right)^2 C_{Y_{\beta}}\right]D\psi + \left(C_{n_{\beta}} - \frac{x}{b} C_{Y_{\beta}}\right)\psi - \left(2\mu K_{XZ} + 2\mu\frac{xz}{b^2} + \right.$$

$$\left. \frac{1}{2}\frac{z}{b} C_{n_{\dot{\beta}}} - \frac{1}{2}\frac{xz}{b^2} C_{Y_{\dot{\beta}}}\right)D^2\phi - \left(\frac{1}{2} C_{n_p} - \frac{1}{2}\frac{x}{b} C_{Y_p} + \frac{z}{b} C_{n_{\beta}} - \frac{xz}{b^2} C_{Y_{\beta}}\right)D\phi + $$

$$\left(\frac{x}{b} C_W\right)\phi = C_{n_O} - \frac{x}{b} C_{Y_O} \tag{11}$$

Rolling-moment equation,

$$\left(-2\mu K_{XZ} - 2\mu\,\frac{xz}{b^2} + \frac{1}{2}\,\frac{x}{b}\,C_{l_{\dot\beta}} + \frac{1}{2}\,\frac{xz}{b^2}\,C_{Y_{\dot\beta}}\right)D^2\psi + \left(\frac{1}{2}\,C_{l_{\dot\beta}} + \frac{1}{2}\,\frac{z}{b}\,C_{Y_{\dot\beta}} - \frac{1}{2}\,C_{l_r} -\right.$$

$$\left.\frac{1}{2}\,\frac{z}{b}\,C_{Y_r} + \frac{x}{b}\,C_{l_\beta} + \frac{xz}{b^2}\,C_{Y_\beta}\right)D\psi + \left(C_{l_\beta} + \frac{z}{b}\,C_{Y_\beta}\right)\psi + \left[2\mu K_X^{\,2} + 2\mu\left(\frac{z}{b}\right)^2 -\right.$$

$$\left.\frac{1}{2}\,\frac{z}{b}\,C_{l_{\dot\beta}} - \frac{1}{2}\left(\frac{z}{b}\right)^2 C_{Y_{\dot\beta}}\right]D^2\phi - \left[\frac{1}{2}\,C_{l_p} + \frac{1}{2}\,\frac{z}{b}\,C_{Y_p} + \frac{z}{b}\,C_{l_\beta} + \left(\frac{z}{b}\right)^2 C_{Y_\beta}\right]D\phi -$$

$$\left(\frac{z}{b}\,C_W + K_\phi\right)\phi = C_{l_0} + \frac{z}{b}\,C_{Y_0} \tag{12}$$

When $\phi_0\,e^{\lambda s}$ is substituted for ϕ and $\psi_0\,e^{\lambda s}$ is substituted for ψ in the equations written in determinant form, λ must be a root of the stability equation:

$$A\lambda^4 + B\lambda^3 + C\lambda^2 + D\lambda + E = 0 \tag{13}$$

where

$$A = 4\mu^2\left[K_X^{\,2}K_Z^{\,2} + \left(\frac{z}{b}\right)^2 K_Z^{\,2} + \left(\frac{x}{b}\right)^2 K_X^{\,2} - K_{XZ}^{\,2} - 2\,\frac{xz}{b^2}\,K_{XZ}\right] +$$

$$\mu\left[\frac{x}{b}\,K_X^{\,2}C_{n_{\dot\beta}} - \left(\frac{x}{b}\right)^2 K_X^{\,2}C_{Y_{\dot\beta}} - \frac{z}{b}\,K_Z^{\,2}C_{l_{\dot\beta}} - \left(\frac{z}{b}\right)^2 K_Z^{\,2}C_{Y_{\dot\beta}} +\right.$$

$$\left.\frac{x}{b}\,K_{XZ}C_{l_{\dot\beta}} - \frac{z}{b}\,K_{XZ}C_{n_{\dot\beta}} + 2\,\frac{xz}{b^2}\,K_{XZ}C_{Y_{\dot\beta}}\right]$$

$$B = 2\mu\left[-\frac{z}{b} K_Z{}^2 C_{l_\beta} - \left(\frac{z}{b}\right)^2 K_Z{}^2 C_{Y_\beta} - \frac{z}{b} K_{XZ} C_{n_\beta} + \frac{x}{b} K_X{}^2 C_{n_\beta} - \left(\frac{x}{b}\right)^2 K_X{}^2 C_{Y_\beta} + \right.$$

$$\left. \frac{x}{b} K_{XZ} C_{l_\beta} + 2\frac{xz}{b^2} C_{Y_\beta} \right] + \mu\left[-K_Z{}^2 C_{l_p} - \left(\frac{x}{b}\right)^2 C_{l_p} - K_{XZ} C_{n_p} - \frac{xz}{b^2} C_{n_p} - \right.$$

$$\frac{z}{b} K_Z{}^2 C_{Y_p} + \frac{x}{b} K_{XZ} C_{Y_p} - K_X{}^2 C_{n_r} - \left(\frac{z}{b}\right)^2 C_{n_r} - K_{XZ} C_{l_r} - \frac{xz}{b^2} C_{l_r} + \frac{x}{b} K_X{}^2 C_{Y_r} -$$

$$\left. \frac{z}{b} K_{XZ} C_{Y_r} + K_X{}^2 C_{n_{\dot\beta}} + \left(\frac{z}{b}\right)^2 C_{n_{\dot\beta}} + K_{XZ} C_{l_{\dot\beta}} + \frac{xz}{b^2} C_{l_{\dot\beta}} - \frac{x}{b} K_X{}^2 C_{Y_{\dot\beta}} + \frac{z}{b} K_{XZ} C_{Y_{\dot\beta}} \right] +$$

$$\frac{1}{4}\left[-\frac{x}{b} C_{n_{\dot\beta}} C_{l_p} + \frac{x}{b} C_{l_{\dot\beta}} C_{n_p} + \left(\frac{x}{b}\right)^2 C_{Y_{\dot\beta}} C_{l_p} - \left(\frac{x}{b}\right)^2 C_{l_{\dot\beta}} C_{Y_p} + \frac{z}{b} C_{l_{\dot\beta}} C_{n_r} - \right.$$

$$\frac{z}{b} C_{l_r} C_{n_{\dot\beta}} + \left(\frac{z}{b}\right)^2 C_{Y_{\dot\beta}} C_{n_r} - \left(\frac{z}{b}\right)^2 C_{n_{\dot\beta}} C_{Y_r} - \frac{xz}{b^2} C_{n_{\dot\beta}} C_{Y_p} - \frac{xz}{b^2} C_{l_{\dot\beta}} C_{Y_r} +$$

$$\left. \frac{xz}{b^2} C_{Y_{\dot\beta}} C_{n_p} + \frac{xz}{b^2} C_{Y_{\dot\beta}} C_{l_r} \right]$$

$$C = 2\mu\left[-K_Z{}^2\left(\frac{z}{b} C_W + C_K\right) + \frac{x}{b} K_{XZ} C_W - \left(\frac{x}{b}\right)^2 C_K + K_X{}^2 C_{n_\beta} + \left(\frac{z}{b}\right)^2 C_{n_\beta} + K_{XZ} C_{l_\beta} + \right.$$

$$\left. \frac{xz}{b^2} C_{l_\beta} - \frac{x}{b} K_X{}^2 C_{Y_\beta} + \frac{z}{b} K_{XZ} C_{Y_\beta} \right] + \frac{1}{2}\left[-\frac{x}{b} C_{n_{\dot\beta}}\left(\frac{z}{b} C_W + C_K\right) - \left(\frac{x}{b}\right)^2 C_{l_{\dot\beta}} C_W + \right.$$

$$\left(\frac{x}{b}\right)^2 C_{Y_{\dot\beta}} C_K - \frac{x}{b} C_{n_\beta} C_{l_p} + \left(\frac{x}{b}\right)^2 C_{Y_\beta} C_{l_p} + \frac{x}{b} C_{l_\beta} C_{n_p} + \frac{xz}{b^2} C_{Y_\beta} C_{n_p} -$$

$$\frac{xz}{b^2} C_{n_\beta} C_{Y_p} - \left(\frac{x}{b}\right)^2 C_{l_\beta} C_{Y_p} + \frac{z}{b} C_{l_\beta} C_{n_r} + \left(\frac{z}{b}\right)^2 C_{Y_\beta} C_{n_r} - \frac{z}{b} C_{n_\beta} C_{l_r} +$$

$$\left. \frac{xz}{b^2} C_{Y_\beta} C_{l_r} - \frac{xz}{b^2} C_{l_\beta} C_{Y_r} - \left(\frac{z}{b}\right)^2 C_{n_\beta} C_{Y_r} \right] + \frac{1}{4}\left[-C_{n_{\dot\beta}} C_{l_p} + \frac{x}{b} C_{Y_{\dot\beta}} C_{l_p} + \right.$$

$$C_{n_r} C_{l_p} - \frac{x}{b} C_{Y_r} C_{l_p} + C_{l_{\dot\beta}} C_{n_p} - C_{l_r} C_{n_p} - \frac{z}{b} C_{Y_r} C_{n_p} + \frac{z}{b} C_{Y_{\dot\beta}} C_{n_p} -$$

$$\left. \frac{z}{b} C_{n_{\dot\beta}} C_{Y_p} + \frac{z}{b} C_{n_r} C_{Y_p} - \frac{x}{b} C_{l_{\dot\beta}} C_{Y_p} + \frac{x}{b} C_{l_r} C_{Y_p} \right]$$

$$D = -\frac{x}{b}C_{n_\beta}\left(\frac{z}{b}C_W + C_K\right) + \left(\frac{x}{b}\right)^2\left(-C_{l_\beta}C_W + C_{Y_\beta}C_K\right) + \frac{1}{2}\left[-C_{n_{\dot\beta}}\left(\frac{z}{b}C_W + C_K\right) + \right.$$

$$C_{n_r}\left(\frac{z}{b}C_W + C_K\right) + \frac{x}{b}\left(C_{l_r}C_W - C_{Y_r}C_K\right) - \frac{x}{b}\left(C_{l_{\dot\beta}}C_W - C_{Y_{\dot\beta}}C_K\right) -$$

$$\left. C_{n_\beta}C_{l_p} + \frac{x}{b}C_{Y_\beta}C_{l_p} + C_{l_\beta}C_{n_p} + \frac{z}{b}C_{Y_\beta}C_{n_p} - \frac{z}{b}C_{n_\beta}C_{Y_p} - \frac{x}{b}C_{l_\beta}C_{Y_p}\right]$$

$$E = -C_{n_\beta}\left(\frac{z}{b}C_W + C_K\right) - \frac{x}{b}\left(C_{l_\beta}C_W - C_{Y_\beta}C_K\right)$$

The following relationships were used to determine the period and time to damp to one-half amplitude from the roots of equation (13):

$$P = \frac{2\pi b}{\omega V}$$

$$T_{1/2} = \frac{0.693b}{aV}$$

where a and ω are the real and imaginary parts of the complex roots $\lambda = a \pm i\omega$.

Calculations of Period and Damping

The period and time to damp to one-half amplitude of the lateral oscillations for the models of the F-84E and F7U-3 airplanes were calculated for the conditions listed in table I. The conventional static-lateral-stability derivatives used in equations (11) and (12) were determined from force tests in the Langley free-flight tunnel and the conventional rotary lateral derivatives used in these equations were estimated by methods presented in reference 4. The values for the moment arms $\left(\frac{x}{b} \text{ and } \frac{z}{b}\right)$ used in these equations are given in the fol-lowing table:

Airplane	Loading	x/b	z/b
F-84E	I II III	0.399 .398 .397	-0.076 -.093 -.111
F7U-3		.488	-.151

For both models, calculations were made for systematic changes in spring restraint in roll corresponding to the springs used in the experimental investigations. For simplicity in discussing the results, the springs were numbered from 1 to 5 and the following table gives the values of the various spring parameters:

Spring	Full-scale spring constant, ft-lb/radian	Value of $C_K + \frac{z}{b} C_W$			
		F-84E loading			F7U-3
		I	II	III	
None	0	-0.0388	-0.049	-0.058	-0.0917
1	100,000	-.1358	-.146	-.155	-------
2	180,000	-------	------	------	-.1762
3	200,000	-.2448	-.255	-.264	-------
4	235,000	-------	------	------	-.2019
5	490,000	-------	------	------	-.3248

The spring-restraint parameter $C_K + \frac{z}{b} C_W$ depends not only on the spring constant but also on the weight of the airplane. In the preceding table, therefore, for the F-84E model there are three values of $C_K + \frac{z}{b} C_W$ for each spring corresponding to the weight at each loading condition.

For the F-84E model, calculations of the period and time to damp to one-half amplitude were also made to show the effect of artificial increases in the damping in yaw for loadings I, II, and III (μ = 18.36, 23.0, and 27.3, respectively) with no roll spring restraint and for the loading III, spring 3 case.

The values of the artificial damping in yaw for the model of the F-84E airplane were calculated from the measured response characteristics of the rate-gyro—servomechanism system and the measured rudder effectiveness. The yaw-damper conditions of the tests were represented as nearly as possible in the calculations by the three different values of artificial damping in yaw which are listed for the model of the F-84E in table I. It should be noted that these values are considerably larger than the first estimates reported in reference 1, which were in error.

Calculation of the Motions

Motions were calculated with the Reeves Electronic Analog Computer (REAC) by using equations (11) and (12) for all the conditions summarized in table I. The disturbances used for these calculations represented the disturbances measured from the test records as nearly as possible. The duration and sequence of the aileron controls used for the calculations corresponded to those measured from the test records. The aileron rolling moments were obtained from force tests of the model.

In the tests of reference 1 for the stable conditions, the F-84E model was disturbed by an abrupt 35° aileron deflection and then the controls were centered for the rest of the test. This disturbance was represented for the REAC calculations by applying a rolling moment corresponding to 35° aileron deflection $\left(C_{l_o} = 0.05\right)$ for 0.2 second. The time of 0.2 second was an approximate value obtained by averaging the values read from the film records for several cases. For the unstable test conditions, the oscillations were started by a gust in the tunnel airstream after the model had been steadied with the controls or with a launching line and then released with the controls fixed for the test record. For the calculations involving unstable oscillations, the gust was represented by a rolling moment one-tenth as large as that used for the stable cases $\left(C_{l_o} = 0.005\right)$.

In the tests of reference 2 for the stable configurations, the oscillations of the F7U-3 were started by alternate left and right aileron controls in phase with the rolling displacement to produce large-amplitude motions. Because the control sequences differed somewhat for the various cases, the control direction and duration were obtained from the film records for each condition and duplicated for the REAC calculations. Rolling and yawing moments corresponding to 30° aileron deflection

$\left(C_{l_0} = 0.024, \quad C_{n_0} + \frac{x}{b} C_{Y_0} = 0.002\right)$ were used for these cases. For the

unstable cases, a single rolling moment $\left(C_{l_0} = 0.02\right)$ was applied for

0.1 second to represent the tunnel gust.

A preliminary comparison of the experimental data with the motions calculated as described in the preceding paragraphs showed that in most cases the calculated initial response was different from that obtained in the tests, apparently because the disturbance used in the calculations did not exactly correspond to that used in the tests. The amplitudes of all the calculated motions were therefore adjusted so that the curve at the first peak following the disturbance (called time 0) matched exactly the experimental records. Mathematically this was equivalent to adjusting the magnitude, but not the duration, of the disturbance. It was felt that this procedure was justified because the primary interest in this investigation was not the initial response to the disturbances but rather the motions following the initial response.

RESULTS AND DISCUSSION

The results of the calculations and the corresponding data obtained from the experiments are presented in figures 2 to 9. The calculated and experimental values of period and damping are compared in figures 2 and 7 for systematic variations of roll spring restraint (as measured by

$C_K + \frac{z}{b} C_W$) for the F-84E and F7U-3 models, respectively. The experimental values of time to damp to one-half amplitude were obtained from test records of references 1 and 2 by taking the average values from the damping envelopes of the first several cycles. The calculated and experimental rolling motions for the same conditions are compared in figure 3 for the F-84E model and in figures 8 and 9 for the F7U-3 model. In the case of all the motions calculated on the REAC, only the rolling motions are presented because only the rolling motions were obtained from the tests of references 1 and 2.

The effect of the yaw damper for various loadings of the F84E model is shown in figure 4 by both the experimental and calculated data. The calculated and experimental motions are compared for the same conditions in figures 5 and 6.

F-84E Results

Effect of roll spring.- For all the F-84E conditions without the yaw damper, the calculations of period and time to damp to one-half amplitude

predict two oscillations which will be designated as the more stable oscillation and the less stable oscillation. Comparison of the calculated and experimental damping values in figure 2 indicates that the oscillation obtained in the tests corresponds to the less stable mode predicted by the calculations, although in a few cases the experimental periods appear to agree more closely with the periods calculated for the more stable oscillation. In general the calculated values of period and time to damp agree with the experimental values for all the conditions shown in figure 2. No experimental value for damping is presented for the loading I, roll spring 3 case because the irregular motion made it impossible to determine the time to damp. The comparison of the test and calculated motions in figure 3, however, shows that the calculations do predict the type of motion for this condition. The slight irregularity in the test record of the loading I, roll spring 1 case in figure 3 appears to be evidence of a short-period oscillation superimposed on the longer period motion but it is not apparent in the calculated motion.

Figure 2 shows that the calculated periods of the two oscillations are usually about the same, except for the loading I case where they become increasingly different with increasing roll spring restraint. This large difference in the periods and the larger initial response of the more stable mode to the disturbance may explain the irregular motion of the loading I, roll spring 3 case. The two modes get out of phase early in the record, and when the amplitude of the stable mode is about the same as that of the less stable mode, the combination produces an unevenly damped motion before the more stable mode disappears. This irregular motion cannot be attributed to the type of control disturbance used because a smooth motion was obtained in the loading II, roll spring 3 case with the same disturbance.

Effect of yaw damper.- The calculations for period and time to damp for the F-84E model with the yaw damper operating predict one oscillation and two very stable aperiodic modes. Figure 4 shows the effect of the yaw damper on the period and damping of the oscillation for the three loading conditions corresponding to values of μ of 18.36 (loading I), 23.0 (loading II), and 27.3 (loading III). Only the values of period and time to damp for the predominant, less stable oscillations of the cases without the yaw damper are presented in figure 4 for comparison with the values for the yaw-damper cases. The calculated aperiodic damping values for the yaw-damper cases are presented in table I. The calculated and experimental motions showing the effect of the yaw damper are compared in figure 5 for the three loading conditions without roll spring restraint and in figure 6 for the loading III, roll spring 3 condition.

The calculations predict the effect of the yaw damper fairly well, although in some cases the quantitative agreement between the test data

and the calculations is not so good. The test and calculated periods shown in figure 4 are only in fair quantitative agreement for loadings II and III but are in qualitative agreement in that both increased with increasing relative-density factor. The test and the calculated damping results are also in qualitative agreement in showing that increases in damping are provided by the yaw damper. Most of the quantitative differ- ence results from the differences between the calculated results and the test points for the no-yaw-damper cases. The calculated and experimental motions in figures 5 and 6 are in qualitative agreement, and the chief differences are in the periods of the calculated and experimental records.

F7U-3 Results

All the calculations made for the F7U-3 model predict two oscilla- tions. The calculated and experimental values for period and time to damp are compared in figure 7. Experimental values for the period are presented for all the conditions, but experimental damping values are presented only for the no-spring condition and for the roll spring 2 case because the irregularity of the motions for the spring 4 and 5 cases makes it very difficult to determine the damping values. The results in figure 7 show that the model had somewhat better damping than that predicted by the calculations for the no-spring condition and for the roll spring 2 case.

The calculated and experimental records for the four spring- restraint conditions are presented in figure 8. As indicated by the data of figure 7, the experimental motions show more damping than the calculated motions for the no-spring condition and for the roll spring 2 case. The comparison of the records for the roll spring 4 and 5 cases shows fairly good agreement between the experimental and calculated motions. In the roll spring 4 case, the calculations predict the same irregular motion in the first three cycles that was found in the exper- imental records.

The data of figure 7 show that the periods of the two oscillations are close for the low-spring-restraint conditions but the periods become increasingly different with increasing spring restraint and, as in the case of the loading I condition for the F-84E model, both the calculated and experimental motions of the F7U-3 model in figure 8 show uneven damping in the first several cycles with roll springs 4 and 5 where the periods of the two predicted modes were most different.

The disturbance sequences were somewhat different for each of the F7U-3 model tests shown in figure 8. In order to verify the results of the F-84E tests which indicated that the type of disturbance was not responsible for the irregular motion, calculations were made for the roll spring 2 case by using the same disturbance as that for the roll

spring 4 case. Results of these calculations are presented in figure 9, together with results for the roll spring 4 case. The data of figure 9 show that the oscillation for the roll spring 2 case is still smoothly damped with this disturbance. It appears, therefore, that, as in the case of the F-84E, the type of disturbance is not the cause of the irregular damping.

The residual motions in figure 8 from about 5 seconds on for the roll spring 4 case and from about 2.5 seconds on for the roll spring 5 case are evidently not oscillations predicted by the calculations. Since the calculations predict good damping for all the modes of these cases, it appears that the residual motions are probably caused by turbulence in the tunnel airstream as suggested in reference 2.

CONCLUSIONS

A theoretical method is presented for predicting the dynamic lateral stability characteristics of an airplane towed in tandem by a much larger airplane. Calculated values of period and time to damp to one-half amplitude and calculated rolling motions have been correlated with results of two experimental investigations conducted in the Langley free-flight tunnel. In general, the theoretical results agree with the experimental results.

Langley Aeronautical Laboratory,
    National Advisory Committee for Aeronautics,
        Langley Field, Va., March 31, 1955.

Robert E. Shanks

Robert E. Shanks
Aeronautical Research Scientist

Approved: *Thomas A. Harris*
    Thomas A. Harris
    Chief of Stability Research Division

dh

NACA RM SL55D18

REFERENCES

1. Shanks, Robert E.: Free-Flight-Tunnel Investigation of the Stability and Control of a Republic F-84E Airplane Towed by a Short Towline. NACA RM SL52K13a, U. S. Air Force, 1952.

2. Grana, David C., and Shanks, Robert E.: Free-Flight-Tunnel Investigation of the Dynamic Stability and Control Characteristics of a Chance Vought F7U-3 Airplane in Towed Flight. NACA RM SL53D07, U. S. Air Force, 1953.

3. Schy, Albert A.: Derivation of the Equations of Motion of a Symmetrical Wing-Tip-Coupled Airplane Configuration With Rotational Freedom at the Junctures. NACA RM L51G12, 1951.

4. Campbell, John P., and McKinney, Marion O.: Summary of Methods for Calculating Dynamic Lateral Stability and Response and for Estimating Lateral Stability Derivatives. NACA Rep. 1098, 1952. (Supersedes NACA TN 2409.)

TABLE I

CONDITIONS FOR WHICH CALCULATIONS WERE MADE, DERIVATIVES USED IN CALCULATIONS, AND RESULTS OF CALCULATIONS

$$\left[c_{Y_{\dot\beta}} = c_{n_{\dot\beta}} = c_{l_{\dot\beta}} = 0 \right]$$

| Loading	Spring	K (full-scale), ft-lb/radian	Yaw damper	$c_K + \frac{z}{b}c_W$	c_{Y_β}	c_{n_β}	c_{l_β}	c_{Y_p}	c_{n_p}	c_{l_p}	c_{Y_r}	c_{n_r}	c_{l_r}	μ	K_X^2	K_Z^2	K_{XZ}	More stable oscillation P, sec	More stable $T_{1/2}$, sec	Less stable oscillation P, sec	Less stable $T_{1/2}$, sec	Aperiodic $T_{1/2}$, sec	Aperiodic $T_{1/2}$, sec
											F-84E												
I	None	--------	None	-0.0388	-0.516	0.103	-0.143	0.010	-0.028	-0.416	0.26	-0.108	0.247	18.36	0.0130	0.0440	-0.0013	1.24	0.08	0.84	-0.38	----	----
	1	100,000		-.1358	-.516	.103	-.143	.010	-.028	-.416	.26	-.108	.247	18.36	.0130	.0440	-.0013	.52	.10	.83	24.40	----	----
	3	200,000		-.2448	-.516	.103	-.143	.010	-.028	-.416	.26	-.108	.247	18.36	.0130	.0440	-.0013	.35	.11	.93	1.42	----	----
II	None	--------	None	-.049	-.516	.103	-.143	.022	-.042	-.416	.26	-.108	.313	23.0	.0492	.0762	-.0023	1.43	.19	1.16	-.34	----	----
	1	100,000		-.146	-.516	.103	-.143	.022	-.042	-.416	.26	-.108	.313	23.0	.0492	.0762	-.0023	1.05	.25	.99	.50	----	----
	3	200,000		-.255	-.516	.103	-.143	.022	-.042	-.416	.26	-.108	.313	23.0	.0492	.0762	-.0023	.81	.48	.94	3.88	----	----
III	None	--------	None	-.058	-.516	.103	-.143	.034	-.056	-.416	.26	-.108	.359	27.3	.0806	.1034	-.0030	1.80	.28	1.49	-.42	----	----
	1	100,000		-.155	-.516	.103	-.143	.034	-.056	-.416	.26	-.108	.359	27.3	.0806	.1034	-.0030	1.43	.30	1.29	-.48	----	----
	3	200,000		-.264	-.516	.103	-.143	.034	-.056	-.416	.26	-.108	.359	27.3	.0806	.1034	-.0030	1.24	.39	1.13	-.72	----	----
I	None	--------	Yes	-.0388	-.516	.103	-.143	.045	-.028	-.416	10.86	-4.32	.247	18.36	.0130	.0440	-.0013			1.04	.52	0.03	0.12
II	None	--------		-.049	-.516	.103	-.143	.071	-.042	-.416	24.66	-9.83	.313	23.0	.0492	.0762	-.0023			1.57	3.22	.02	.30
III	None	--------		-.058	-.516	.103	-.143	.095	-.056	-.416	19.76	-7.88	.359	27.3	.0806	.1034	-.0030			1.97	-3.12	.04	.31
III	3	200,000		-.264	-.516	.103	-.143	.095	-.056	-.416	19.76	-7.88	.359	27.3	.0806	.1034	-.0030			1.03	3.03	.04	.45
											F7U-3												
	None	--------	None	-0.0917	-0.401	0.080	-0.103	-0.050	-0.038	-0.240	0.241	-0.140	0.134	23.3	0.027	0.055	-0.0058	1.13	0.16	1.00	-0.31	----	----
	2	180,000		-.1762	-.401	.080	-.103	-.050	-.038	-.240	.241	-.140	.134	23.3	.027	.055	-.0058	.73	.36	.90	5.08	----	----
	4	235,000		-.2019	-.401	.080	-.103	-.050	-.038	-.240	.241	-.140	.134	23.3	.027	.055	-.0058	.61	.43	.99	1.60	----	----
	5	490,000		-.3248	-.401	.080	-.103	-.050	-.038	-.240	.241	-.140	.134	23.3	.027	.055	-.0058	.42	.43	1.15	1.59	----	----
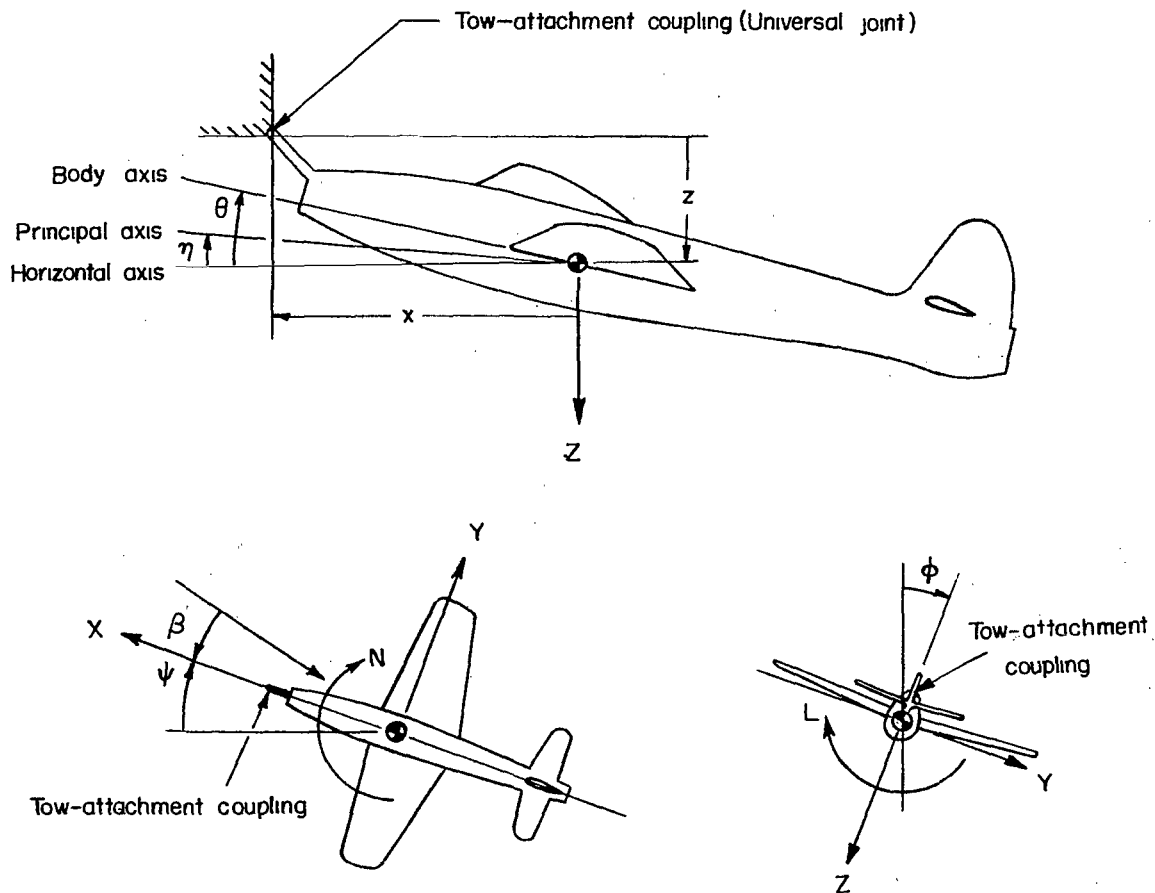
Figure 1.- The stability system of axes. Arrows indicate positive direc-
tions of moments, forces, and angles. This system of axes is defined
as an orthogonal system having the origin at the center of gravity and
in which the Z-axis is in the plane of symmetry and perpendicular to
the relative wind, the X-axis is in the plane of symmetry and perpen-
dicular to the Z-axis, and the Y-axis is perpendicular to the plane of
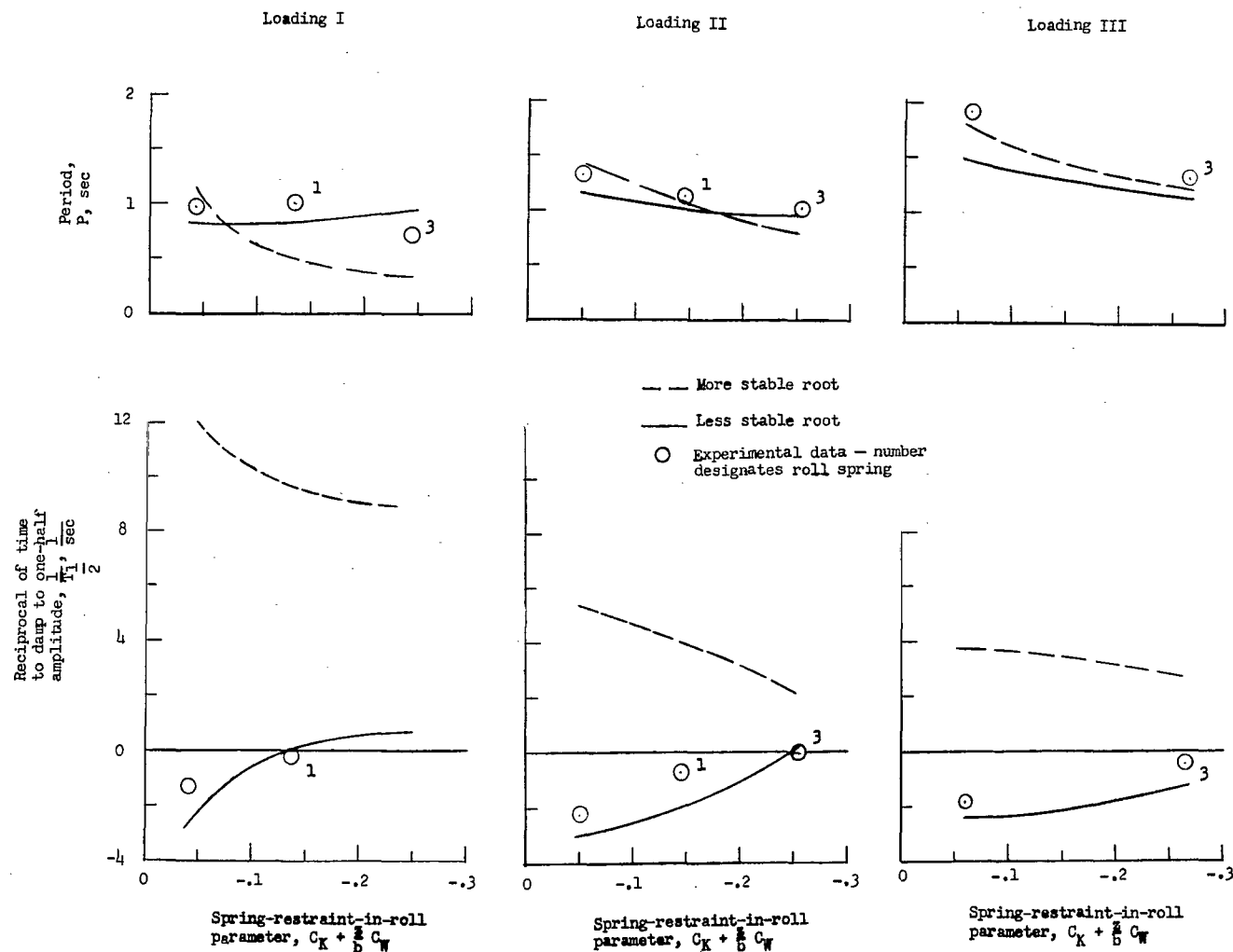symmetry. At a constant angle of attack, these axes are fixed in the
airplane.

Figure 2.- Correlation of period and damping of the model of the F-84E air-
plane for various roll-spring-restraint conditions as obtained from tests
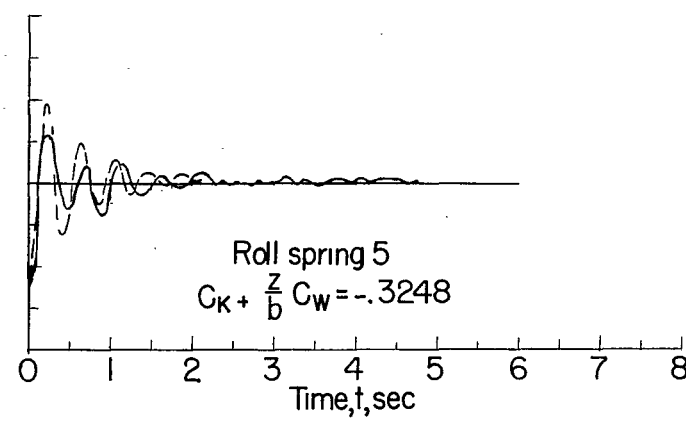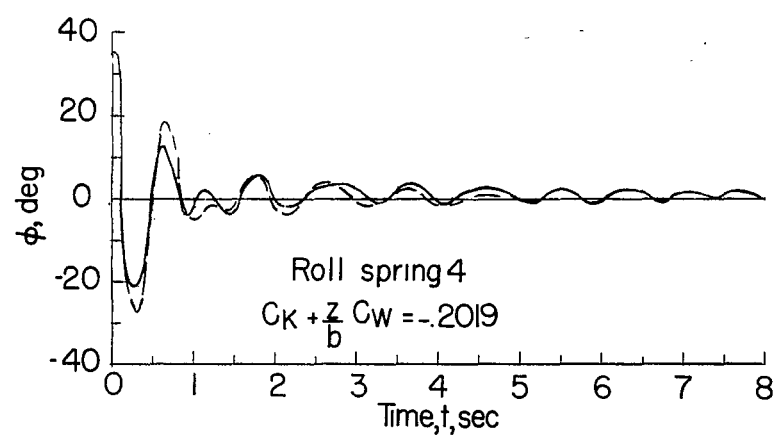and theory. No yaw damper.
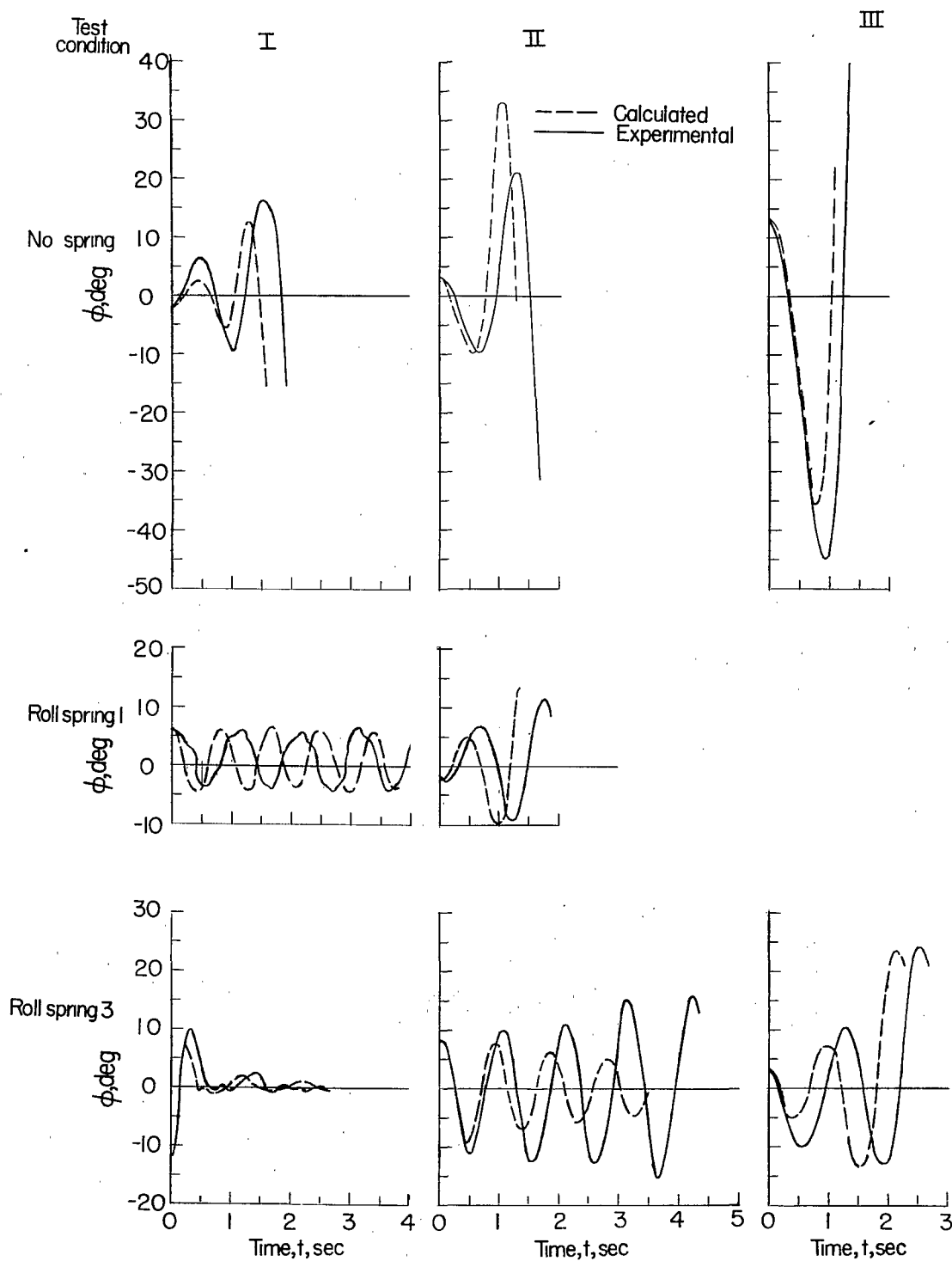
Figure 3.- Comparison of calculated and measured rolling motions for various amounts of spring restraint in roll for the F-84E airplane model. No yaw damper.
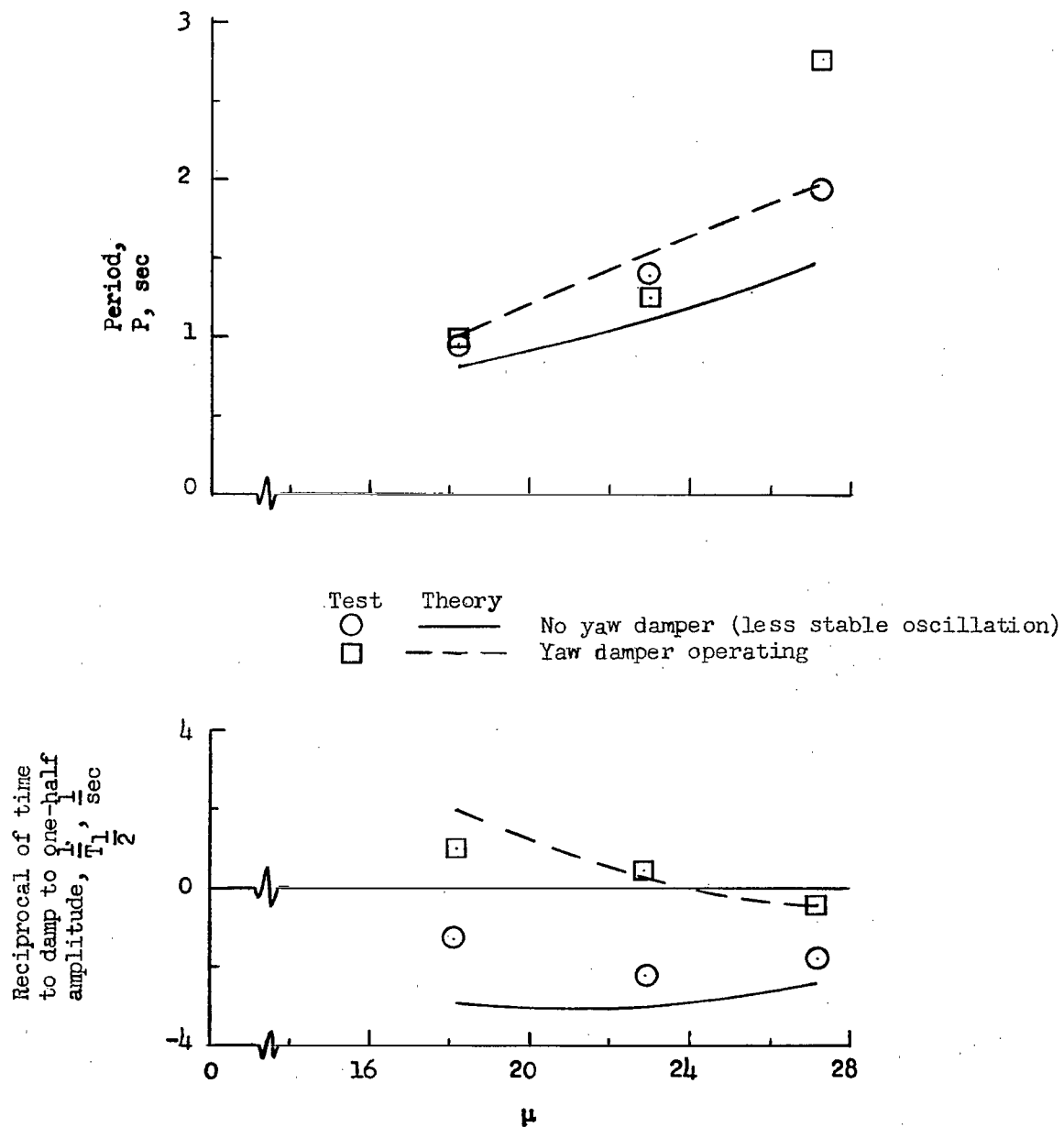
Figure 4.- Effect of the yaw damper on the period and damping of the model of the F-84E airplane for various loadings. No roll springs.
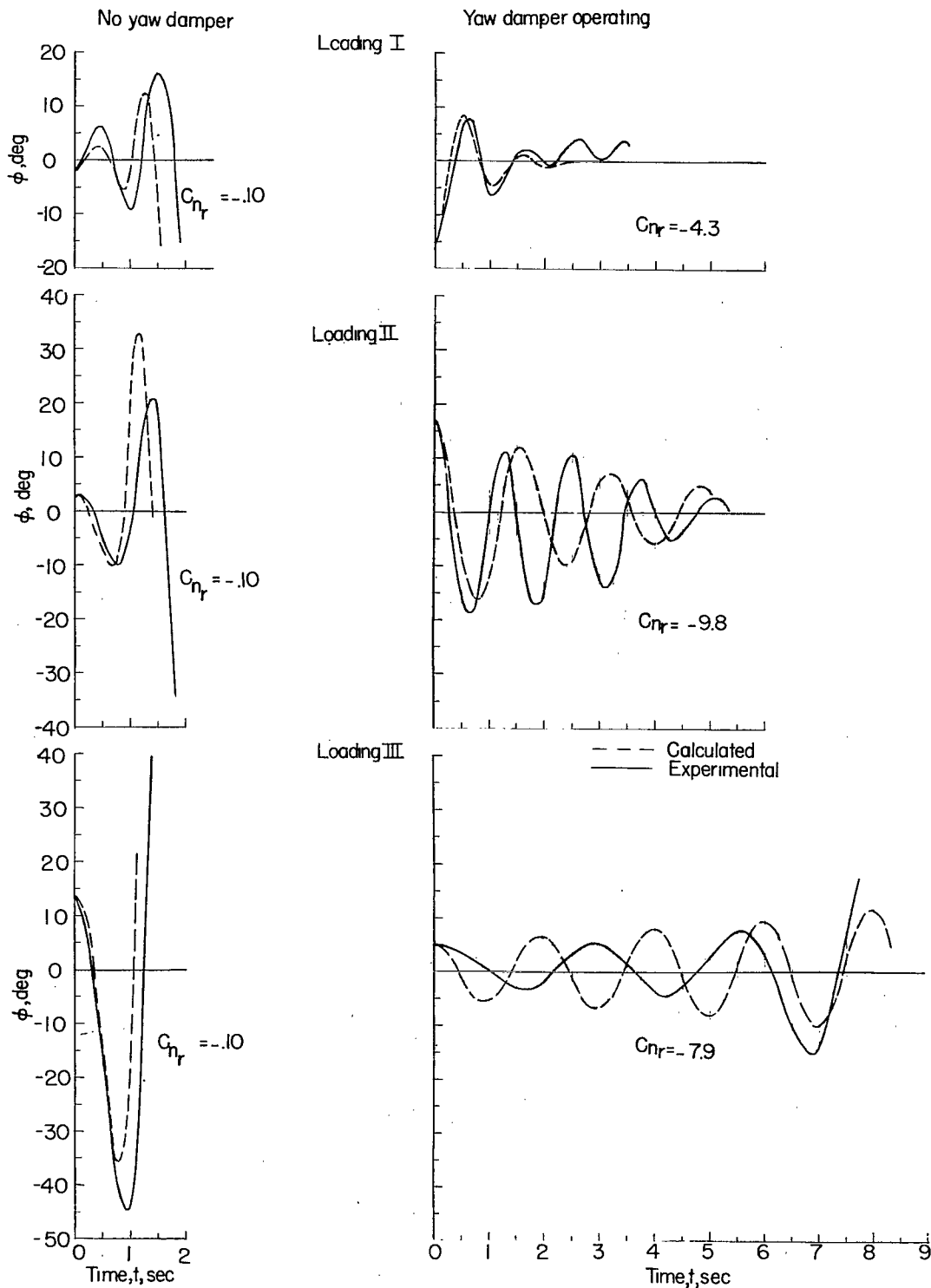
Figure 5.- Effect of yaw damper on the rolling motions as determined by tests and calculations.

No yaw damper
$C_{n_r} = -.11$

$-- -$ Calculated
———— Experimental

Yaw damper operating
$C_{n_r} = -7.9$
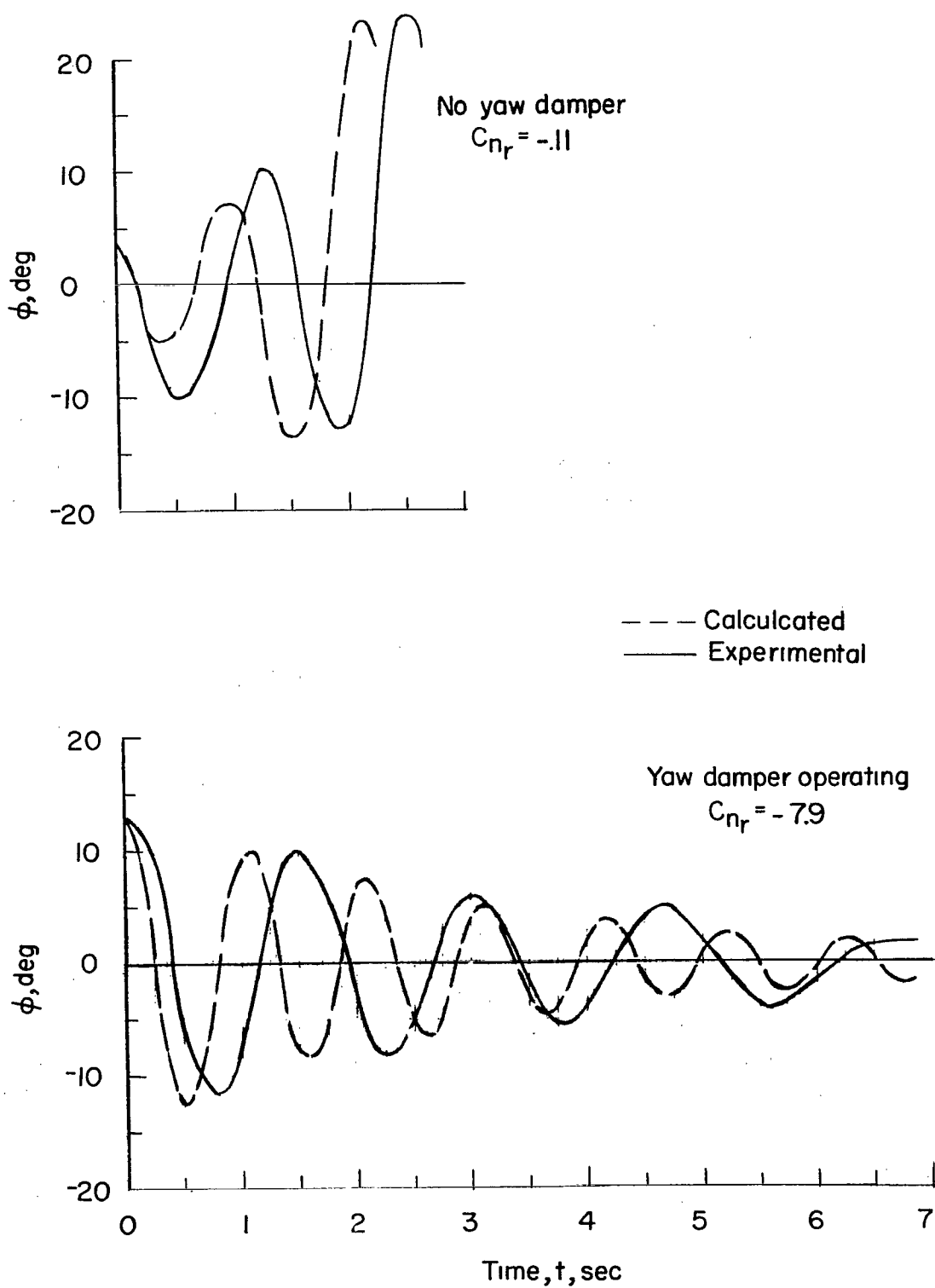
Figure 6.- Effect of the yaw damper on the calculated and measured motions of the F-84E model in the loading III, roll spring 3 condition.
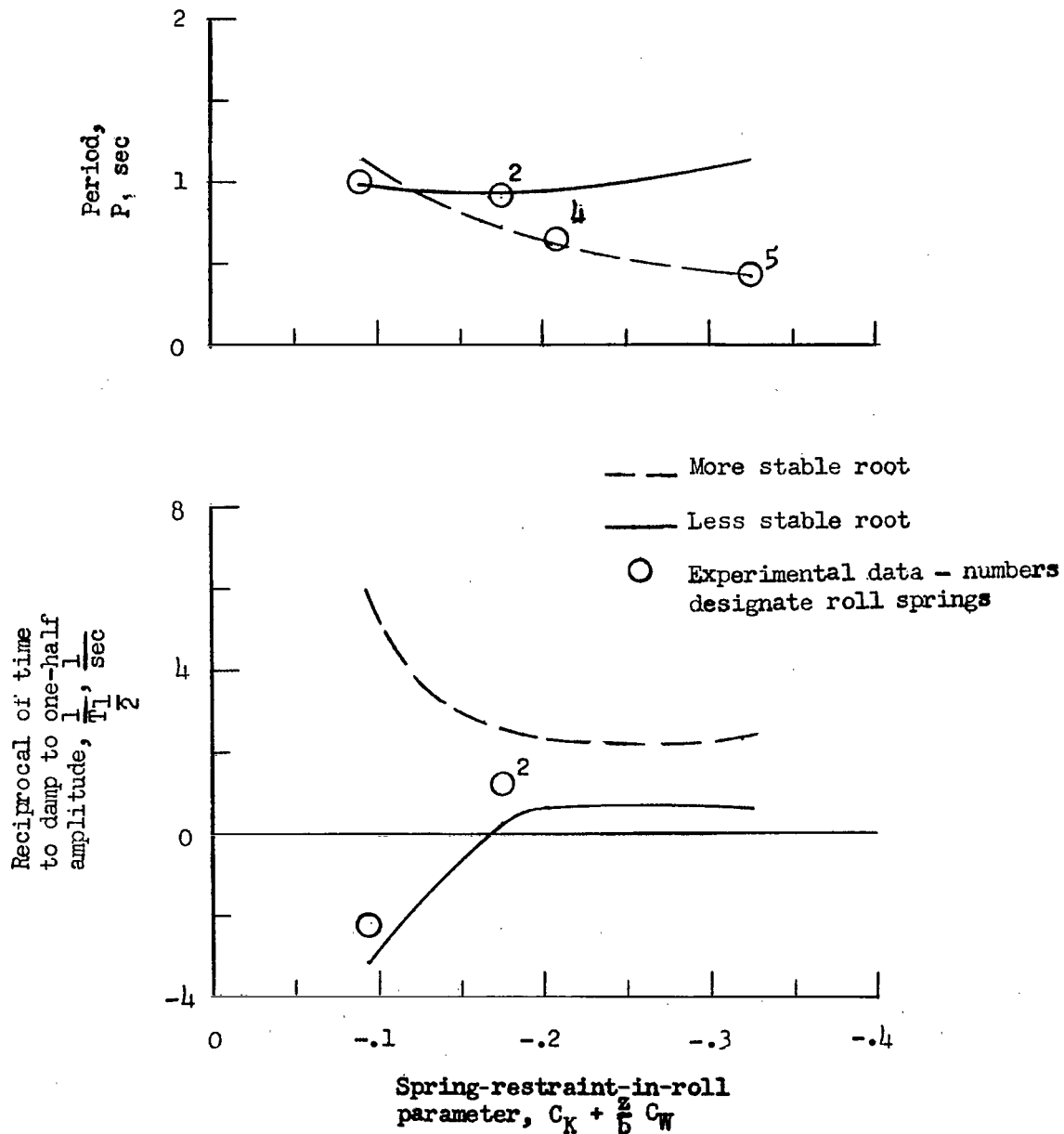
Figure 7.- Correlation of the period and the time to damp to one-half
  amplitude of the rolling oscillations of the model of the F7U-3 air-
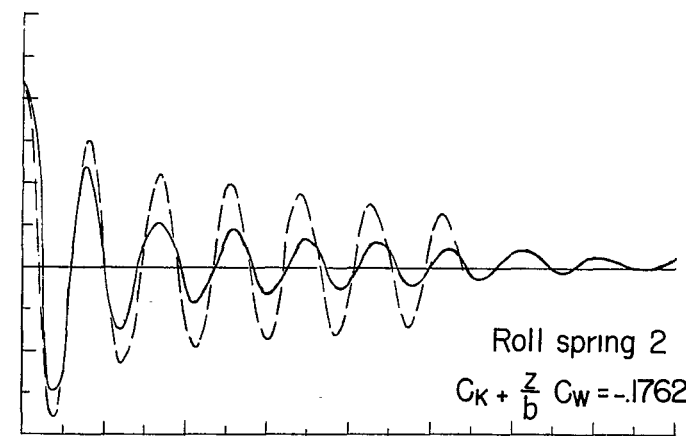 plane for various roll-spring-restraint conditions as obtained from
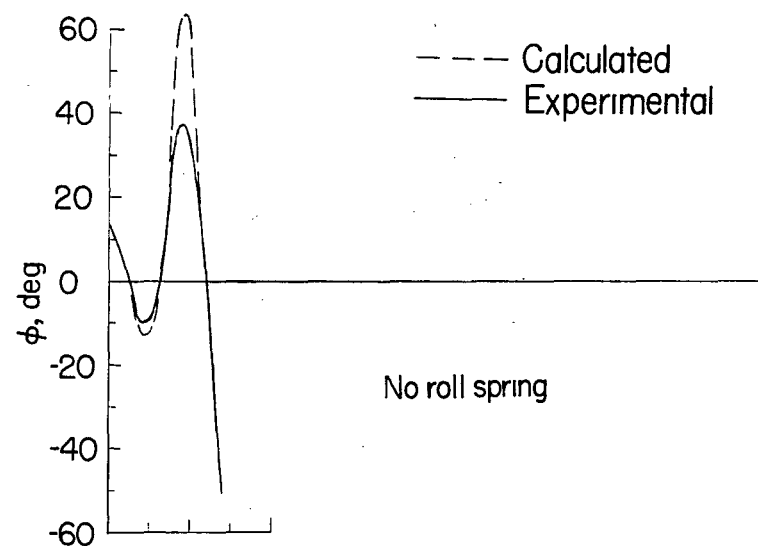 tests and theory.

Figure 8.- Comparison of calculated and measured motions for various amounts of spring restraint in roll for the F7U-3 airplane model.
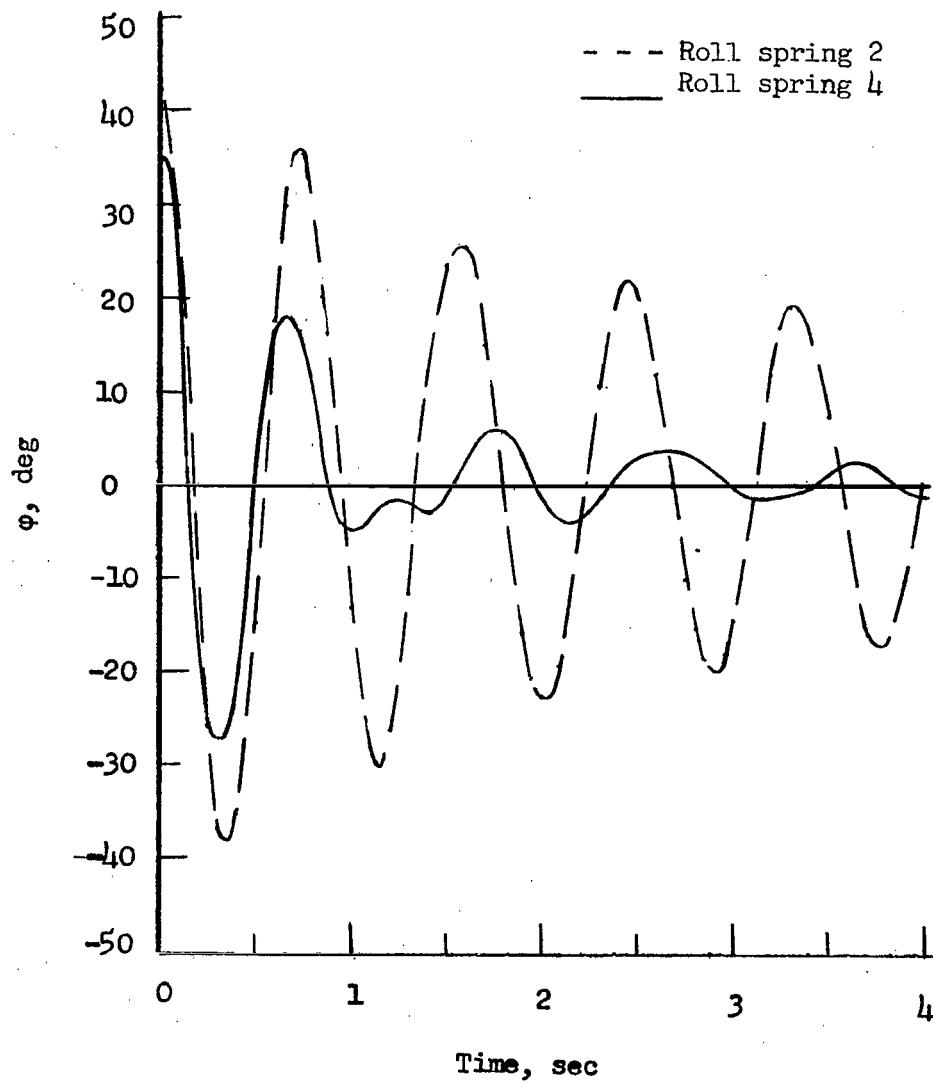
Figure 9.- Comparison of calculated motions for two roll-spring-restraint conditions following the same disturbance sequence for the F7U-3 model.